ACS APPLIED MATERIALS & INTERFACES

Research Article

www.acsami.org

Multifunctional Nanoplatforms for Targeted Multidrug-Resistant-Bacteria Theranostic Applications

Xuemei Dai,[†] Zhen Fan,[†] Yuefeng Lu,[‡] and Paresh Chandra Ray*[,†]

[†]Department of Chemistry, Jackson State University, Jackson, Mississippi 39217, United States

[‡]Department of Neurobiology & Anatomical Science, University of Mississippi Medical Center, Jackson, Mississippi 39216, United States

ABSTRACT: The emergence of multidrug-resistant-bacteria (MDRB) infection poses a major burden to modern healthcare. Early detection in the bloodstream and a new strategy development for MDRB infection treatment without antibiotics are clinically significant to save millions of lives every year. To tackle the MDRB challenge, the current manuscript reports the design of "multifunctional nanoplatforms" consisting of a magnetic core−plasmonic shell nanoparticle, a methylene blue-bound aptamer, and an MDRB Salmonella DT104 specific antibody. The reported "multifunctional nanoplatform" is capable of targeted separation from a blood sample and sensing and multimodal therapeutic killing of MDRB. Experimental data using an MDRB-infected whole-blood sample show that nanoplatforms can be used for selective magnetic separation and fluorescence imaging. In vitro light-triggered photodestruction of MDRB, using combined photodynamic and photothermal treatment, shows that the multimodal treatment regime can enhance MDRB killing significantly. We discussed the possible mechanisms on combined synergistic therapy for killing MDRB. The "multifunctional nanoplatform" reported in this manuscript has great potential for the imaging and combined therapy of MDRB in clinical settings.

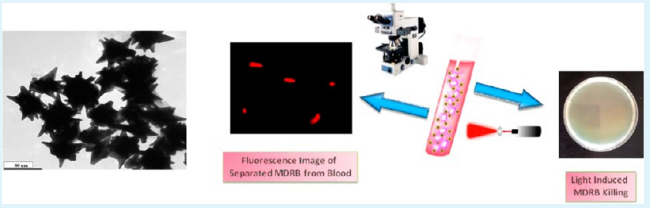

KEYWORDS: *multifunctional nanoplatforms, theranostic core−shell nanostar, MDRB separation from blood, MDRB detection, fluorescence imaging, combined synergistic therapy*

INTRODUCTION

The field of "theranostic multifunctional nanoplatforms", which is still in the early stages of its development, holds huge promise for our society.[1−8] Through the combination of diagnostic and therapeutic capabilities into a single pharmaceutical agent, multifunctional nanoplatforms have the capability of being excellent materials for diagnostic and therapeutic use in cancer and infection disease tretament.[9−14] After the development of penicillin in the 1940s, antibiotics have been used as "miraculous drugs" in clinical practice.[15−20] Because antibiotics have been excessively used in human, veterinary, and agricultural medicine, several bacterial strains have become resistant to numerous antibiotics.[21−27] Over the last decade, several pathogens, including Salmonella DT104, have acquired multidrug resistance to several market-available antibiotics.[19−21] Although the amount of MDRB is continuing to rise day by day, unfortunately, the amount of new antibiotics introduced into the clinical market has declined significantly.[20−27] This clearly indicates that the need for the development of new approaches to cure infection disease is very urgent.[28−38] To tackle this challenge, the current manuscript reports the design of "multifunctional nanoplatforms" that have the capability for combined theranostic applications. We have shown that multifunctional nanoplatforms designed by us have the capability of targeted separation and selective fluorescence imaging of Salmonella DT104 from a blood sample, followed by selective photodestruction. The combination of "photothermal and photodynamic" therapies for the treatment of MDRB infection has been implemented, as reported in Scheme 1. Combination therapy approach will have huge advantages, and these are (1) the expectation of synergistic effects and (2) prevention of the emergence of drug-resistant bacteria. Because in the initial stage of infection the amount of MDRB present in the bloodstream is extremely low, early stage detection of MDRB in the presence of blood mononuclear cells is a real challenge in clinical practice.[16−21] Here we demonstrate that our "multifunctional nanoplatforms" can be used for the separation, imaging, and synergistic photodestruction of MDRB selectively from a whole-blood sample.

EXPERIMENTAL SECTION

Materials. We purchased hydrogen tetrachloroaurate, iron chloride, trisodium citrate, $NaBH_4$, and sodium citrate from Sigma-Aldrich and whole rabbit blood from Colorado Serum Company. We obtained MDRB Salmonella DT104 from the American Type Culture Collection.

Synthesis of Theranostic Multifunctional Nanoplatforms. We synthesized "theranostic multifunctional nanoplatforms" through a

Received: August 23, 2013
Accepted: October 19, 2013
Published: October 20, 2013

Scheme 1. (A) Schematic Diagram Illustrating the Capability of "Multifunctional Nanoplatforms" in Theranostic Nanomedicine, (B) Scheme Showing MDRB Separation Using a Bar Magnet after "Theranostic Nanoplatform" Attachment with Bacteria, and (C) Scheme Illustrating the Possibility of Imaging Using a Fluorescence Microscope and Targeted Light-Induced MDRB Killing after Magnetic Separation Using a "Theranostic Nanoplatform"

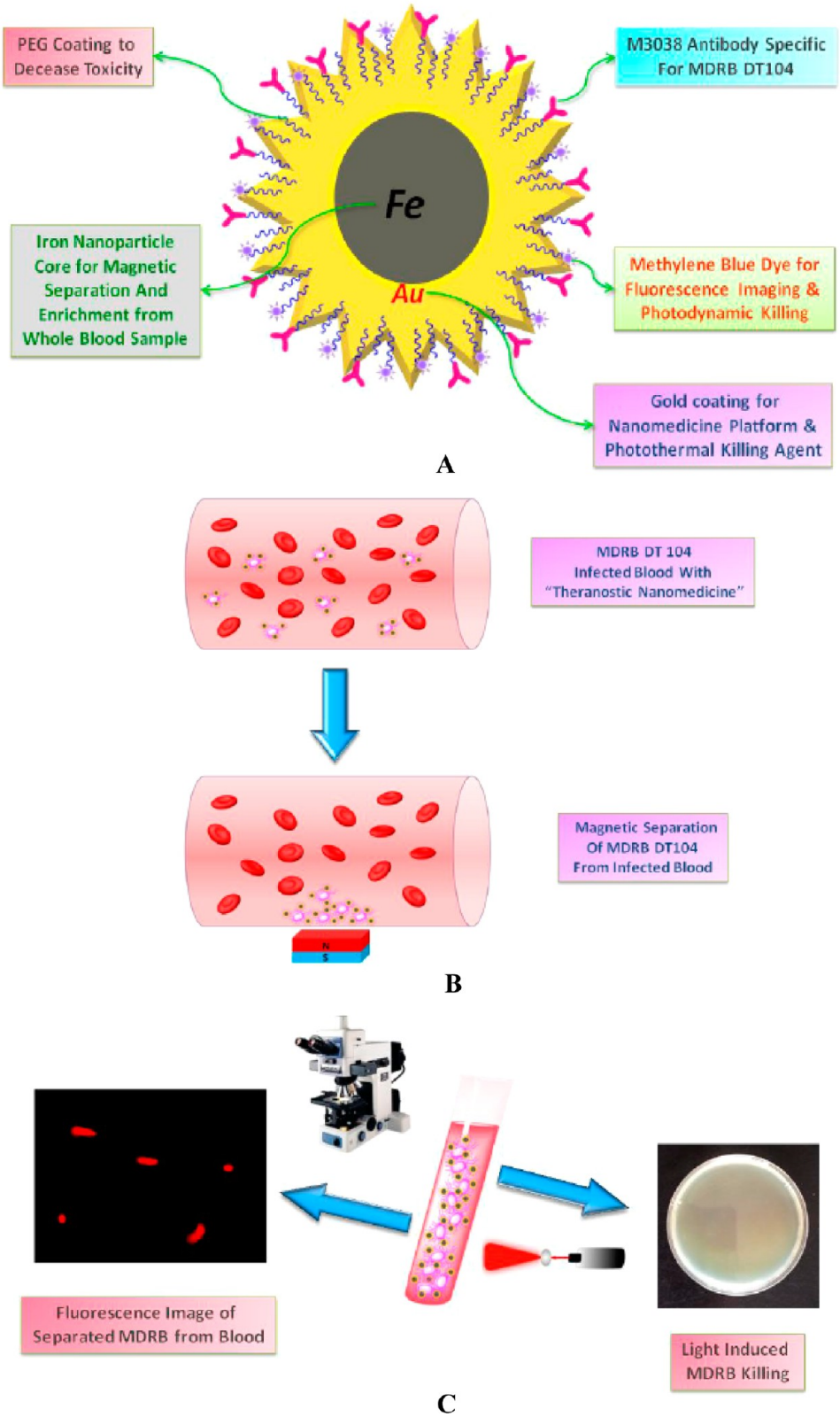

several-step process. At first, a spherical iron nanoparticle was synthesized from $FeCl_3$ using our reported method.[6] We characterized the freshly prepared spherical nanoparticle using a JEM-2100F transmission electron microscope and absorption spectroscopy. As

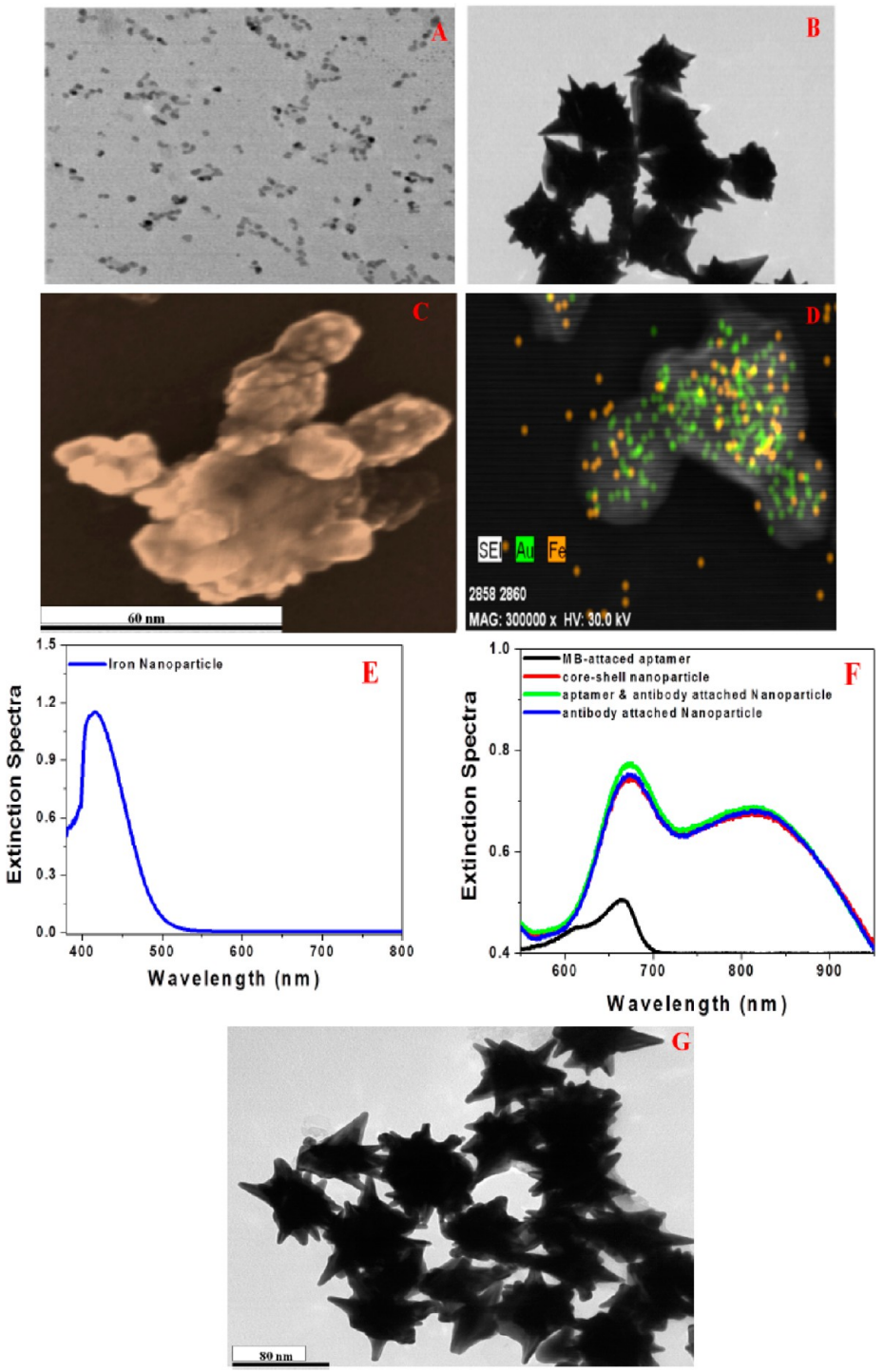

Figure 1. (A) TEM image showing the size of our freshly prepared magnetic nanoparticle. (B) Electron microscopy image of a freshly prepared core−shell nanoparticle, which clearly shows spikes. (C) SEM image also showing the spikes on the nanoparticle, which indicate star-shaped core−shell nanoparticle formation. (D) EDX mapping analysis of star-shaped nanoparticles. (E) Absorption spectra of an iron magnetic nanoparticle synthesized from F_3Cl_3. (F) Absorption spectra of a star-shaped nanoparticle, an MB-bound aptamer, and multifunctional nanoplatforms. (G) TEM image of a freshly prepared MB-bound aptamer and M3038 antibody-attached nanoplatforms.

shown in Figure 1A, our synthesized iron nanoparticle size is about 10 nm. In the next step, a star-shaped magnetic core−gold shell nanoparticle was synthesized in the presence of cetyltrimethylammonium bromide using our reported method.[6] Parts B, C, and F of Figure 1 show the transmission electron microscopy (TEM), scanning electron microscopy (SEM), and UV−visible spectral characterization of freshly prepared star-shaped magnetic core−gold shell nanoparticles. As shown in Figure 1B,C, the star-shaped core−shell nanoparticle size is around 70 nm. Similarly, parts E and F of Figure 1 show the plasmon bands around 650 and 800 nm due to the formation of a gold shell. As shown in Figure 1D, our energy-dispersive X-ray (EDX) mapping experiment clearly shows both iron and gold peaks.

Next, the star-shaped nanoparticle was coated with thiolated poly(ethylene glycol) (PEG) to minimize the nonspecific interaction with blood cells. After that, we attached a monoclonal M3038 antibody on the star-shaped nanoparticle surface for the selective separation of

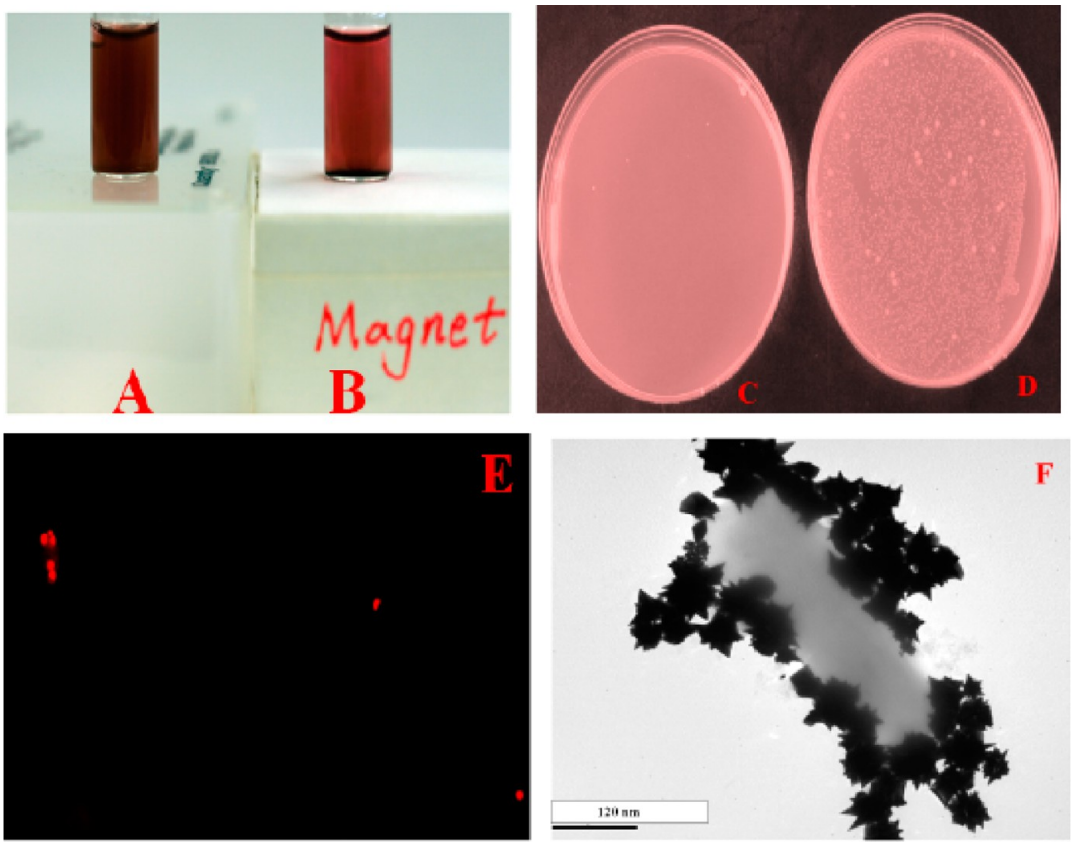

Figure 2. (A) Picture showing no MDRB separation without a magnet. (B) Separation of an MDRB-attached "multifunctional nanoplatform" by a bar magnet. (C) Colonies showing the absence of MDRB Salmonella DT104 in a supernatant solution. (D) Colonies demonstrating the presence of MDRB Salmonella DT104 in a suspension of nanoplatform-conjugated MDRB after magnetic capture and resuspension in PBS. The initial number of MRSA cases were 10^4 CFU/mL. (E) Fluorescent images of MDRB Salmonella DT104 after separation from an infected blood sample. (F) TEM image demonstrating an antibody-conjugated MDRB-attached nanoplatform after magnetic separation.

Salmonella DT104.[16] We also modified the surface using methylene blue (MB)-attached S8-7 aptamers for photodynamic killing. After PEGylation, for aptamer conjugation, thiol-modified S8-7 aptamers were introduced on star-shaped nanoparticles over a 16-h period in the presence of phosphate-buffered saline (PBS) and 0.1 M sodium chloride. Next, unbound aptamers were removed by centrifugation at 6000 rpm for several minutes. After that, the number of aptamer molecules bound in each gold nanoparticle were determined using 10 μM potassium cyanide, which can oxidize the nanoplatform completely. From fluorescence analysis data, we estimated that around 100 aptamers are attached with one nanoparticle.

Next, we attached an M3038 antibody on a "theranostic multifunctional nanoparticle" using cystamine dihydrochloride and reported the glutaraldehyde spacer method,[16,19−21]. Parts F and G of Figure 1 show the absorption spectra and TEM image of a multifunctional nanoplatform. Our data indicate that, during attachment of PEG, aptamer containing MB, and M3038 antibody, the nanoparticle morphology remain unchanged. To understand how stable the multifunctional nanoplatform is, we performed TEM and absorption chracterization once a week for a few weeks and noted that the "multifunctional nanoplatform" developed by us was highly stable even after 1 month.

Bacteria Incubation with a "Multifunctional Nanoplatform". MDRB Salmonella DT104 bacteria was cultured using ATCC protocol, as we reported previously.[24,33,36] Next, "multifunctional nanoplatforms" were mixed with MDRB-infected blood at room temperature with gentle shaking. Then, we used a bar magnet for the magnetic separation experiment. The MDRB separation efficiency was monitored using colony counting.

Fluorescence Analysis. An Olympus IX71 inverted confocal fluorescence microscope has been used for fluorescence imaging after magnetic separation.

PTT, PDT, Combined Killing, and Percentage of Live Bacteria Determination. For phototriggered killing by photodynamic (PDT), photothermal (PTT), or combined therapies, we used 670 nm light from a portable OEM laser, with 1−2 W/cm^2 power. For all phototriggered experiments, we used exactly the same wavelength and the same power. Next, the amount of live bacteria was counted with a colony counter after 24 h at 37 °C incubation.

Reactive Oxygen Species (ROS) Generation Measurement. We used a singlet oxygen sensor green reagent (SOSG; Sigma) for measurement of the ROS formation during treatment. For measurement of the SOSG fluorescence intensity, we used a microplate reader. An excitation wavelength of 485 nm was used for fluorescence excitation, and the emission wavelength was recorded at 528 nm.

RESULTS AND DISCUSSION

As shown in Scheme 1, in multifunctional nanoplatforms designed by us, core magnetic nanoparticles were used for circulating MDRB separation and enrichment from blood samples. A gold shell allows conjugation of a biorecognition agent via gold−sulfur chemistry for selective separation and imaging. Also, a star-shaped gold coating will help to stabilize the high-magnetic-moment nanoparticles in blood and eliminate possible toxicity from an iron nanoparticle. Because gold nanoparticles are well-known to generate high temperatures in the presence of near-infrared (NIR) light,[39−48] in our design, a gold coating was used also as an "optical nanoheater".

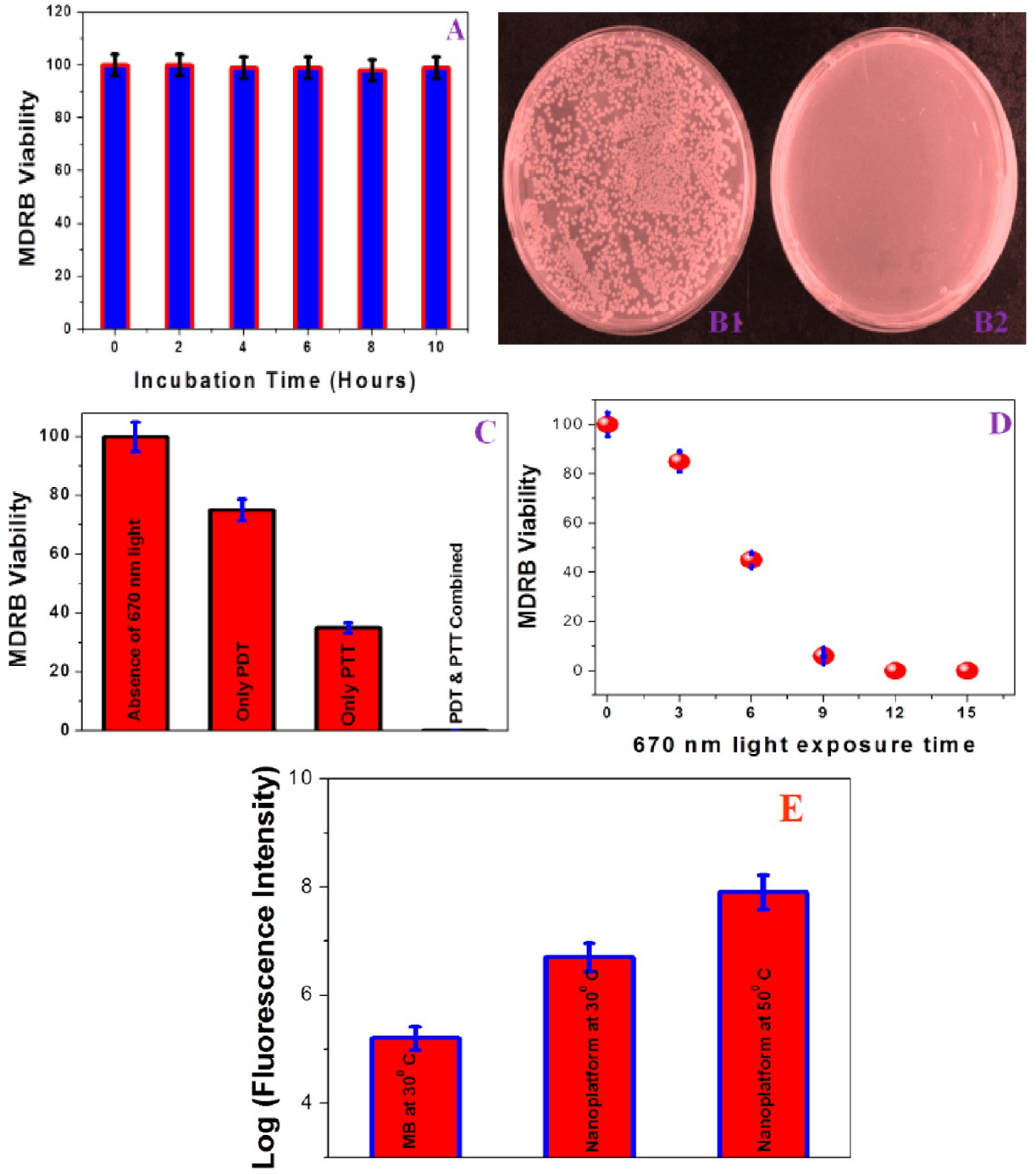

Figure 3. (A) Plot showing that the MDRB viability is 100% in the absence of 670 nm light even after 10 h of incubation in the presence of a "multifunctional nanoplatform". (B) Colonies of MDRB Salmonella DT104 bacteria after combined therapy for 12 min. (B1) Combined therapy in the absence of a "multifunctional nanoplatform". (B2) Combined therapy in the presence a "multifunctional nanoplatform". (C) Plot showing the MDRB viability after 12 min of 670 nm laser exposure, in the case of PDT, PTT, and combined therapies. (D) Plot demonstrating the time-dependent combined therapy efficiency. (E) Plot showing how the fluorescence intensity from SOSG varies in the presence of a "multifunctional nanoplatform" during combined therapy.

As shown in Figure 1G, our developed MB-attached nanoplatform exhibited strong absorption at 670 nm; we used MB as a dual probe for NIR fluorescence imaging using 670 nm light excitation and as a PDT sensitizer platform. In PDT, light-activated photosensitizers generate ROS, which can irreversibly damage cancerous cells and tissues.[49−59] Because MB is a well-known PDT drug,[49−51] a multifunctional nanoplatform can be used for 670 nm light-induced PDT and PTT together.

Next, to understand whether a "multifunctional nanoplatform" can be used for selective MDRB detection in a clinical setting, MDRB Salmonella DT104 bacteria were spiked into the whole rabbit blood suspension at different concentrations. After 120 min of gentle shaking, we incubated a few microliter nanoplatform with 1 mL of a Salmonella DT104 suspension in blood containing 10^4 CFU/mL for 20 min. Next, MDRB-attached nanoplatforms were separated and enriched using a bar magnet, and during this process, we enriched the

concentration 20 times. As shown in Figure 2, we used bacteria colony counting and TEM and fluorescence imaging techniques to characterize suspensions of the nanoplatform−MDRB conjugates and supernatants. Our bacteria-counting-colony data, as shown in Figure 2C, show no MDRB Salmonella DT104 present in the supernatant. As a result, our experimental data show that most of the MDRB are conjugated with a "multifunctional nanoplatform" and separated by the magnet. Parts D and E of Figure 2 shows the colonies and fluorescence images of MDRB Salmonella after magnetic separation. As one can see from Figure 2F, several nanoplatforms were conjugated with one Salmonella bacteria through antogen−antibody interaction. All of the above characterizations indicate that our developed "multifunctional nanoplatform" is highly selective for binding with MDRB Salmonella DT104 and has the capability of separating MDRB from the blood sample even at a concentration of 0.01% cell mixtures. Our result indicates that the magnetic capture efficiency of the nanoplatform is about 97% for MDRB from an infected blood sample.

Next, to determine whether a "multifunctional nanoplatform" can be used for the combined synergistic photodestruction of MDRB, we have used 670 nm light irradiation experiments. To understand whether combined PTT and PDT is much superior to a single therapy, we designed several different experiments. At first, an MDRB-attached "multifunctional nanoplatform" was incubated for 10 h without any laser light to find possible cytotoxicity. As shown in Figure 3A, about 100% MDRB viability was observed even after 10 h of incubation, which indicates that our theranostic nanoplatform is not cytotoxic in the absence of external NIR light. Next, we used an M3038 antibody-conjugated nanoparticle without MB, in the presence of external 670 nm light, to find out the contribution from only PTT. After that, to evaluate both PTT and PDT contributions in the presence of 670 nm light, we used an MB-bound aptamer and an M3038 antibody-conjugated nanoplatform. At the end, we used aptamer-conjugated MB without a nanoparticle, in the presence of external 670 nm light, to find only the PDT contribution. In all cases, we used 670 nm light at 1−2 W/cm^2 power at different time intervals. Parts B−D of Figure 3 clearly indicate that 100% of MDRB was dead, just after 12 min of treatment of combined therapy. Next, we performed a thermal imaging experiment to measure how the temperature increases during photothermal destruction in the presence of 670 nm light. For this purpose, we used a MikroShot Camera for recording thermal imaging data at 1 min intervals. Experimental results indicate that the temperature was increased to about 48 °C when an MDRB-attached "multifunctional nanoplatform" was exposed to 1−2 W/cm^2 power 670 nm light. We have also noted that, at exactly the same laser power and wavelength, the temperature was increased to about 32 °C in the absence of a multifunctional nanoplatform.

Parts B−D of Figure 3 also clearly show that it will take about 12 min to kill 100% of MDRB when we performed the combined therapy, whereas 68% of MDRB were killed after 12 min of treatment in the case of only PTT. On the other hand, only 25% were killed even after 12 min of PDT treatment. So, our data clearly indicate that the MDRB viability was remarkably reduced under combined treatment and the MDRB killing rate is much higher than that by PDT or PTT separately. Our experimental data demonstrate a significant synergistic therapeutic effect for MDRB killing using combined treatment.

Because MB can generate ROS during 670 nm light irradiation to kill MDRB, the PDT efficiency should be highly dependent on the ROS formation capability. Recently, it has been reported that ROS formation from photosensitizers can be enhanced in the presence of plasmonic gold nanoparticles.[54−59] Previous results also indicate enhancement of the ROS formation during PTT due to temperature enhancement.[54−59] As a result, to found out the possible mechanism for the synergistic effect during combined therapy, we used SOSG to find the amount of ROS formation enhancement during a laser-induced therapy process. Figure 3E shows how the SOSG fluorescence intensity varies during PTT in the presence of a multifunctional nanoplatform. Our results indicate 1.25 times more ROS formation in the presence of a "multifunctional nanoplatform". Our experimental observation on more ROS formation can be due to the presence of a plasmonic field on the sharp corner of a multifunctional nanoparticle. We also noted that ROS formation increased another 1.2 times during PTT because of the temperature increment during PTT. As a result, we observed a significant synergistic therapeutic effect for MDRB killing using combined treatment. Our reported experiment demonstrated that the multimodal (PTT and PDT together) treatment can enhance in vitro MDRB therapy significantly because of the synergistic therapeutic effect.

CONCLUSION

The current manuscript reports the design of a "multifunctional nanoplatform" consisting of a magnetic core−plasmonic shell nanoparticle, a MB-bound aptamer, and a MDRB-specific antibody, which can be used for synergistic theranostic applications. Our results show that a "multifunctional nanoplatform" is capable of targeted separation and sensing and multimodal therapeutic killing of MDRB in a single procedure. Our results with a 0.01% MDRB-infected blood sample show that a nanoplatform can be used for selective imaging after magnetic separation. Our experimental data have shown that a multifunctional nanoplatform developed by us can be used for combined synergistic therapy using PTT and PDT together. We have demonstrated that combined treatment can be highly effective for in vitro MDRB killing. We have shown that ROS formation by a MB photosensitizer can be enhanced during PTT because of the presence of a nanoplatform and elevation of the temperature. Although our developed "multifunctional nanoplatform"-based reported results are very exciting, we admit that we are now in the initial stage of development. We believe that this "multifunctional nanoplatform" wiil have enormous potential as a clinical sample once it has been optimized in clinical settings.

AUTHOR INFORMATION

Corresponding Author

*E-mail: paresh.c.ray@jsums.edu. Fax: 601-979-3674.

Notes

The authors declare no competing financial interest.

ACKNOWLEDGMENTS

We are grateful to NSF-PREM (Grant DMR-0611539) for their generous funding.

REFERENCES

(1) Ma, X.; Zhao, Y.; Liang, X. J. *Acc. Chem. Res.* **2011**, *44*, 1114−1122.

(2) Lammers, T.; Aime, S.; Hennink, W. E.; Storm, G.; Kiessling, F. *Acc. Chem. Res.* **2011**, *44*, 1029−38.
(3) Li, Y.; Ma, J.; Zhu, H.; Gao, X.; Dong, H.; Shi, D. *ACS Appl. Mater. Interfaces* **2013**, *5*, 7227−7235.
(4) Cabral, H.; Nishiyama, N.; Kataoka, K. *Acc. Chem. Res.* **2011**, *44*, 999−1008.
(5) Kelkar, S. S.; Reineke, T. M. *Bioconjugate Chem.* **2011**, *22*, 1879.
(6) Fan, Z.; Senapati, D.; Singh, A. K.; Ray, P. C. *Mol. Pharmaceutics* **2013**, *10*, 857−866.
(7) Jokerst, J. V.; Gambhir, S. S. *Acc. Chem. Res.* **2011**, *44*, 1050−1060.
(8) Wang, H.; Wu, Y.; Zhao, R.; Nie, G. *Adv. Mater.* **2013**, *25*, 1616−1622.
(9) Cho, N. H.; Cheong, T. C.; Min, J. H.; Wu, J. H.; Lee, S. J.; Kim, D.; Yang, J. S.; Kim, S.; Kim, Y. K.; Seong, S. Y. *Nat. Nanotechnol.* **2011**, *6*, 675−82.
(10) Yoo, D.; Lee, J. H.; Shin, T. H.; Cheon, J. *Acc. Chem. Res.* **2011**, *44*, 863−874.
(11) Narayanan, S.; Sathy, B. N.; Mony, U.; Koyakutty, M.; Nair, S. V.; Menon, D. *ACS Appl. Mater. Interfaces* **2012**, *4*, 251−260.
(12) Bardhan, R.; Lal, S.; Joshi, A.; Halas, N. J. *Acc. Chem. Res.* **2011**, *44*, 936−946.
(13) Saha, K.; Agasti, S. S.; Kim, C.; Li, X.; Rotello, V. M. *Chem. Rev.* **2012**, *112*, 2739−2779.
(14) Dong, W. J.; Li, Y. S.; Niu, D. C.; Ma, Z.; Gu, J. L.; Chen, Y.; Zhao, W. R.; Liu, X. H.; Liu, C. S.; Shi, J. L. *Adv. Mater.* **2011**, *23*, 5392−5397.
(15) Andersson, D. I.; Hughes, D. *Nat. Rev.* **2010**, *8*, 260−271.
(16) Ronholm, J.; Zhang, Z.; Cao, X.; Lin, M. *Hybridoma* **2011**, *30*, 43−52.
(17) Zhang, Q. C.; Lambert, G.; Liao, D.; Kim, H.; Robin, K.; Tung, C. K.; Pourmand, N.; Austin, R. H. *Science* **2011**, *333*, 1764−1767.
(18) Zhang, Q.; Robin, K.; Liao, D.; Lambert, G.; Austin, R. H. *Mol. Pharmaceutics* **2011**, *8*, 2063−2068.
(19) Allen, H. K.; Donato, J.; Wang, H. H.; Cloud-Hansen, K. A.; Davies, J.; Handelsman, J. *Nat. Rev. Microbiol.* **2010**, *8*, 251−259.
(20) Miranda, O. R.; Li, X.; Garcia-Gonzalez, L.; Zhu, Z.-J.; Yan, B.; Bunz, U. H. F.; Rotello, V. M. *J. Am. Chem. Soc.* **2011**, *133*, 9650−9653.
(21) Dwivedi, H. P.; Smiley, R. D.; Jaykus, L. A. *Appl. Microbiol. Biotechnol.* **2013**, *97*, 3677−86.
(22) Kaki, R.; Elligsen, M.; Walker, S.; Simor, A.; Palmay, L. *J. Antimicrob. Chemother.* **2011**, *66*, 1223−1230.
(23) Hayden, S. C.; Zhao, G.; Saha, K.; Phillips, R. L.; Li, X.; Miranda, O. R.; Rotello, V. M.; El-Sayed, M. A.; Schmidt-Krey, I.; Bunz, U. H. F. *J. Am. Chem. Soc.* **2012**, *134*, 6920−6923.
(24) Fan, Z.; Senapati, D.; Khan, S. A.; Singh, A. K.; Hamme, A.; Yust, B.; Sardar, D.; Ray, P. C. *Chem.—Eur. J.* **2013**, *19*, 2839−2847.
(25) Khan, S. A.; Singh, A. K.; Senapati, D.; Fan, Z.; Ray, P. C. *Chem. Soc. Rev.* **2012**, *41*, 3193−3209.
(26) Berry, V.; Gole, A.; Kundu, S.; Murphy, C. J.; Saraf, R. F. *J. Am. Chem. Soc.* **2005**, *127*, 17600−17602.
(27) Norman, R. S.; Stone, J. W.; Gole, A.; Murphy, C. J.; Sabo-Attwood, T. L. *Nano Lett.* **2008**, *8*, 302−306.
(28) Wang, C.; Irudayaraj, J. *Small* **2008**, *4*, 2204−2208.
(29) Zharov, V. P.; Mercer, K. E.; Galitovskaya, E. N.; Smeltzer, M. S. *Biophys. J.* **2006**, *90*, 619−627.
(30) Singh, A. K.; Senapati, D.; Wang, S.; Griffin, J.; Neely, A.; Candice, P.; Naylor, K. M.; Varisli, B.; Kalluri, J. R.; Ray, P. C. *ACS Nano* **2009**, *3*, 1906−1912.
(31) Wang, S.; Singh, A. K.; Senapati, D.; Neely, A.; Yu, H.; Ray, P. C. *Chem.—Eur. J.* **2010**, *16*, 5600−5606.
(32) Nair, A. S.; Binoy, N. P.; Ramakrishna, S.; Kurup, T. R.; Chan, L. W.; Gosh, C. H.; Md. Islam, M. R.; Utschig, T.; Pradeep, T. *ACS Appl. Mater. Interfaces* **2009**, *1*, 2413−2419.
(33) Khan, S. A.; Singh, A. K.; Senapati, D.; Fan, Z.; Ray, P. C. *Chem. Commun.* **2011**, *47*, 9444−9446.
(34) Levin, C. S.; Hoffman, C.; Ali, T. A.; Kelly, A. T.; Morosan, E.; Nordlander, P.; Whitmire, K. H.; Halas, N. J. *ACS Nano* **2009**, *3*, 1379−1388.
(35) Tang, J.; Chen, Q.; Xu, L.; Zhang, S.; Feng, L.; Cheng, L.; Xu, H.; Liu, Z.; Peng, R. *ACS Appl. Mater. Interfaces* **2013**, *5*, 3867−3874.
(36) Khan, S. A.; Singh, A. K.; Senapati, D.; Fan, Z.; Ray, P. C. *J. Mater. Chem.* **2011**, *21*, 17705−17709.
(37) Kell, A. J.; Stewart, G.; Ryan, S.; Peytavi, R.; Boissinot, B.; Huletsky, A.; Bergeron, M. G.; Simard, B. *ACS Nano* **2008**, *2*, 1777−1788.
(38) Ray, P. C. *Chem. Rev.* **2010**, *110*, 5332−5365.
(39) Huang, X.; El-Sayed, I. H.; Qian, W.; El-Sayed, M. A. *J. Am. Chem. Soc.* **2006**, *128*, 2115−2120.
(40) Singh, A. K.; Lu, W.; Senapati, D.; Khan, S. A.; Fan, Z.; Senapati, T.; Demeritte, T.; Beqa, L.; Ray, P. C. *Small* **2011**, *7*, 2517−2525.
(41) Lu, W.; Singh, A. K.; Khan, S. A.; Senapati, D.; Yu, H.; Ray, P. C. *J. Am. Chem. Soc.* **2010**, *132*, 18103−18114.
(42) Kaittanis, C.; Santra, S.; Perez, J. M. *J. Am. Chem. Soc.* **2009**, *131*, 12780−12791.
(43) Liu, H. L.; Hua, M. Y.; Yang, H. W.; Huang, C. Y.; Chu, P. C.; Wu, J. S.; Tseng, I. C.; Wang, J. J.; Yen, T. C.; Chen, P. Y.; Wei, K. C. *Proc. Natl. Acad. Sci. U.S.A.* **2010**, *107*, 15205−15210.
(44) Li, F.; Zhao, Q.; Wang, C.; Lu, X.; Li, X. F.; Le, X. C. *Anal. Chem.* **2010**, *82*, 3399−3403.
(45) Dreaden, E. C.; Alkilany, A. M.; Huang, X.; Murphy, C. J.; El-Sayed, M. A. *Chem. Soc. Rev.* **2012**, *41*, 2740−2779.
(46) Beqa, L.; Fan, Z.; Singh, A. K.; Senapati, D.; Ray, P. C. *ACS Appl. Mater. Interfaces* **2011**, *3*, 3316−3324.
(47) Lu, W.; Arumugam, S. R.; Senapati, D.; Singh, A. K.; Arbneshi, T.; Khan, S. A.; Yu, H.; Ray, P. C. *ACS Nano* **2010**, *4*, 1739−1749.
(48) Schmucker, A. L.; Harris, N.; Banholzer, M. J.; Blaber, M. G.; Osberg, K. D.; Schatz, G. C.; Mirkin, C. A. *ACS Nano* **2010**, *4*, 5453−5463.
(49) Noimark, S.; Dunnill, C. W.; Kay, W. M. C.; Perni, S.; Prokopovich, P.; Ismail, S.; Wilson, M.; Parkin, I. V. *J. Mater. Chem.* **2012**, *22*, 15388−15396.
(50) Usacheva, M. N.; Teichert, M. C.; Biel, M. A. *J. Photochem. Photobiol. B* **2003**, *71*, 87−98.
(51) Tang, W.; Xu, H.; Park, E. J.; Philbert, M. A.; Kopelman, R. *Biochem. Biophys. Res. Commun.* **2008**, *369*, 579−83.
(52) Tada, B. D.; Vono, L. R.; Duarte, L. E.; Itri, R.; Kiyohara, P. K.; Baptista, M. S.; Rossi, L. M. *Langmuir* **2007**, *23*, 8194−8199.
(53) Celli, J. P.; Spring, B. Q.; Rizvi, I.; Evans, C. L.; Samkoe, K. S.; Verma, S.; Pogue, B. W.; Hasan, T. *Chem. Rev.* **2010**, *110*, 2795−2838.
(54) Tian, B.; Wang, C.; Zhang, S.; Feng, L.; Liu, Z. *ACS Nano* **2011**, *5*, 7000−7009.
(55) Jin, C. S.; Lovell, J. F.; Chen, J.; Zheng, G. *ACS Nano* **2013**, *7*, 2541−2550.
(56) Yu, J.; Javier, D.; Yaseen, M. A.; Nitin, N.; Richards-Kortum, R.; Anvari, B.; Wong, M. S. *J. Am. Chem. Soc.* **2010**, *132*, 1929−1938.
(57) Wang, J.; Zhu, G.; You, M.; Song, E.; Shukoor, M. I.; Zhang, K.; Altman, M. B.; Chen, Y.; Zhu, Z.; Huang, C. Z.; et al. *ACS Nano* **2012**, *6*, 5070−5077.
(58) Jang, B.; Park, J. Y.; Tung, C. H.; Kim, I. H.; Choi, Y. *ACS Nano* **2011**, *5*, 1086−1094.
(59) Wang, J.; Zhu, G.; You, M.; Song, E.; Shukoor, M. I.; Zhang, K.; Altman, M. B.; Chen, Y.; Zhu, Z.; Huang, C. Z. *ACS Nano* **2012**, *6*, 5070−5077.